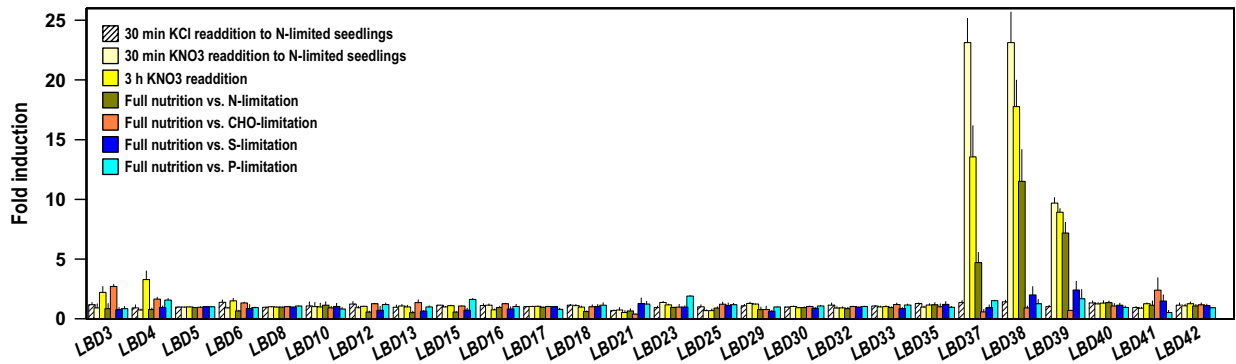


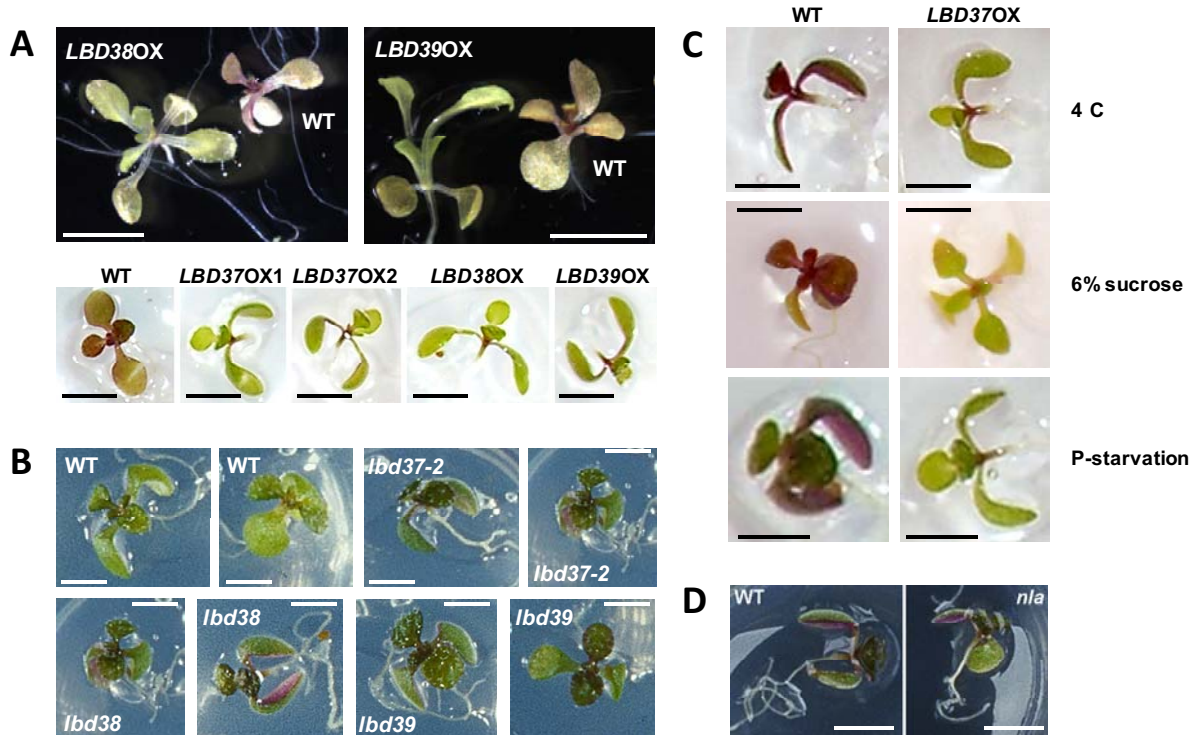
Supplemental Figure 1. Nitrate-specific, strong induction of *LBD37*, *LBD38*, *LBD39*.

Shown are induction levels of all *LBD* genes represented on the ATH1 GeneChip® (data from Scheible *et al.*, 2004; Morcuende *et al.*, 2007, Osuna *et al.*, 2007, data for sulfur-depletion unpublished). The bars depict the change of transcript level in N-limited seedlings 30 min after re-addition of 3 mM KCl (white hatched), 30 min after re-addition of 3 mM KNO₃ (light yellow), 3 h after re-addition of 3 mM KNO₃ (full yellow), and of nutrient-replete seedlings versus N-limited seedlings (dark yellow). Orange, blue and cyan bars show the change in the comparison of nutrient-replete seedlings versus carbohydrate (CHO), sulfur (S) and phosphorous (P)-limited seedlings, respectively. Data are from two biological replicates for each condition. Mean values and standard deviations (n=4) are shown and were calculated from crosswise comparisons of the biological replicates (cond. A repl 1 vs. cond. B repl. 1; cond. A repl 2 vs. cond. B repl. 1; cond. A repl 2 vs. cond. B repl. 2).



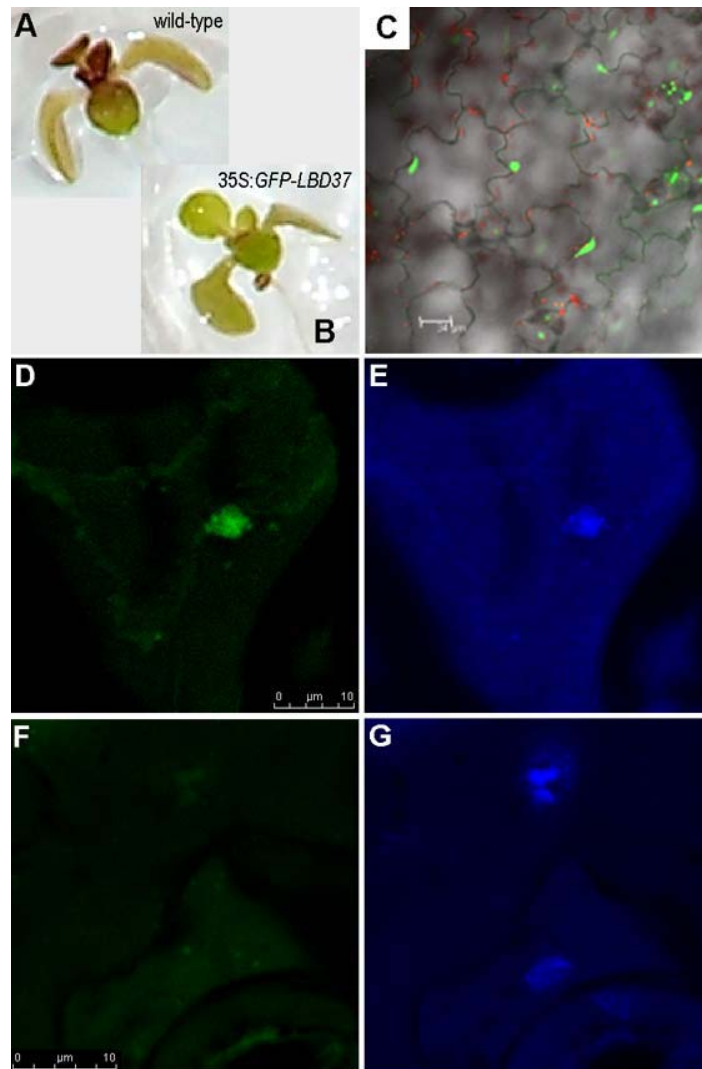
Supplemental Figure 2. Anthocyanin pigmentation phenotypes.

(A) Nine-day-old, N-limited WT and N-limited *LBD37*, *38* or *39* over-expressing seedlings. Photographs from independent experiments (top row, 2nd row) are shown. For *LBD37* over-expressers, two independent lines are shown in the second row. **(B)** Nine-day-old, nitrate-replete WT and nitrate-replete *lbd37-2*, *38* and *39* mutant seedlings. Two representative photos of different individuals are shown for each genotype. **(C)** Nine-day-old WT and *LBD37* OX seedlings grown in the cold (4°C), in the presence of 6% sucrose or under P-starvation conditions. **(D)** Nine-day-old, N-limited WT and N-limited *nla* mutant seedlings. Bars = 4 mm.



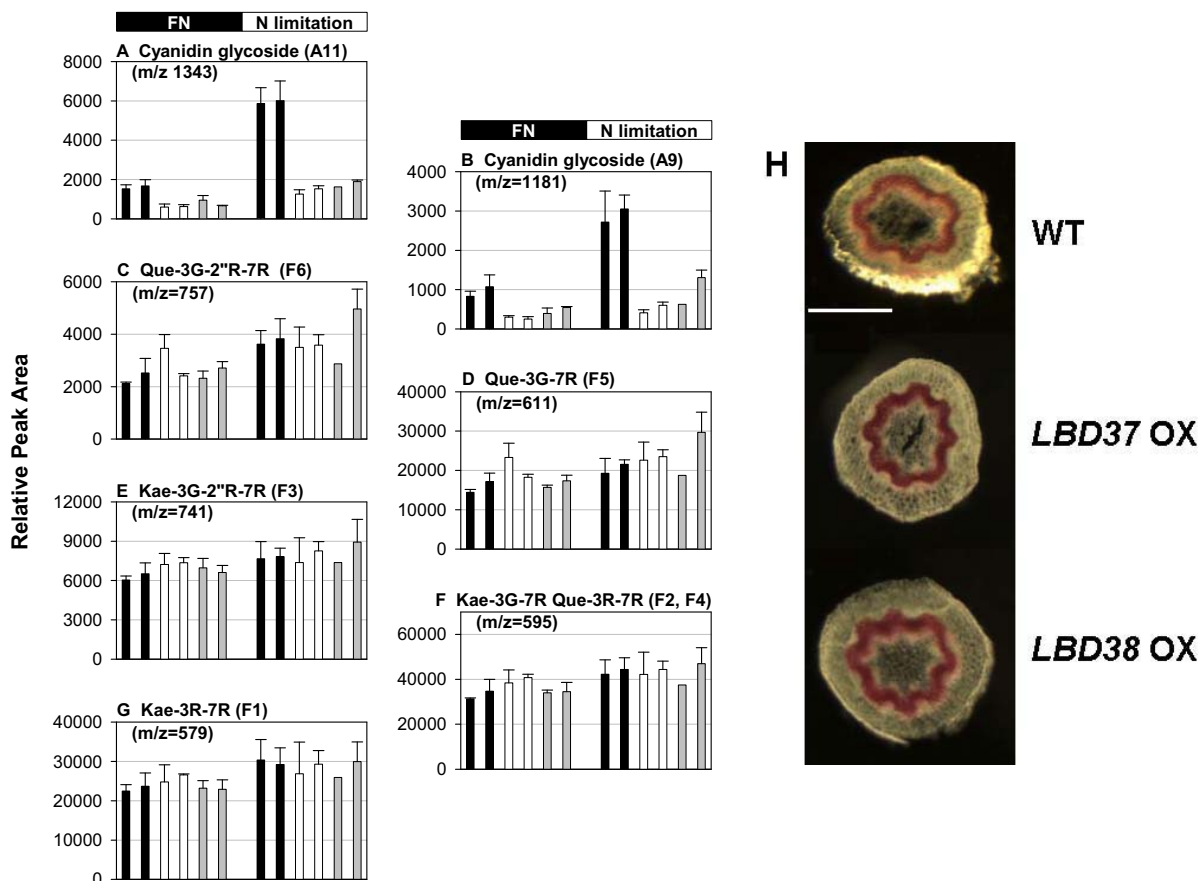
Supplemental Figure 3. Nuclear localization of GFP-LBD37 fusion protein.

(A, B) Compared to N-limited WT (A) N-limited seedlings expressing GFP-LBD37 under control of the 35S CaMV promoter (B) display reduced anthocyanin levels. (C) GFP signal and chlorophyll fluorescence in leaf epidermal cells of a *35S:GFP-LBD37* line. The size of the scale bar is 34 μm . (D) GFP signal in the nucleus of a *35S:GFP-LBD37* leaf mesophyll cell. (E) DAPI staining of the same cell as in (D). (F) no GFP signal is detected in the negative control i.e. WT leaf mesophyll cells. (G) DAPI staining of the tissue sample shown in (F). The full sizes of the scale bars in (D) and (F) are 10 μm , and apply to (E) and (G), respectively.



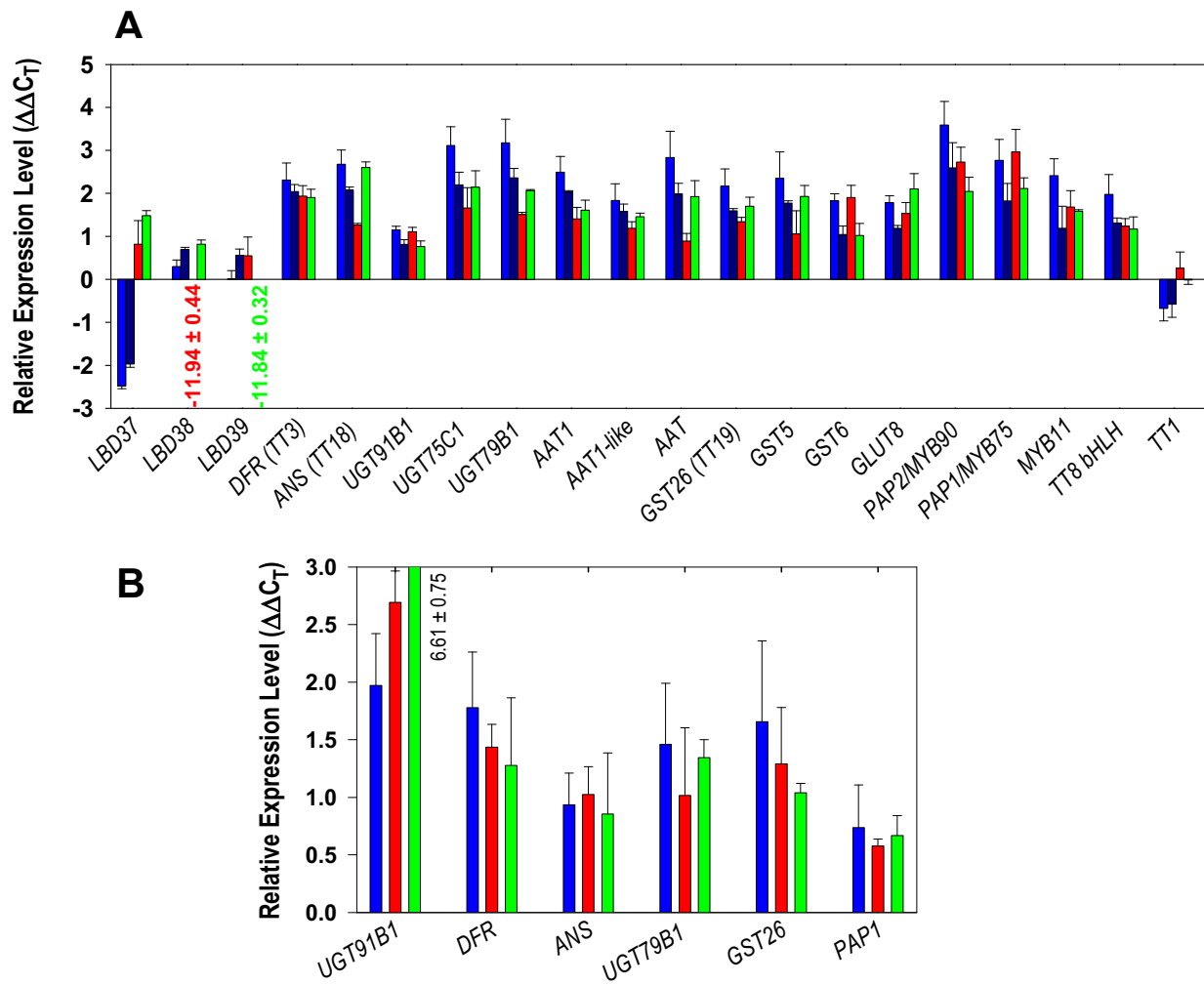
Supplemental Figure 4. Flavonoid levels and lignin staining.

Contents of seven detected cyanidin and flavonol glycoside species in shoot-material from NO_3^- -fed (FN, black horizontal bar) and N-limited (N limitation, white horizontal bar) WT (black vertical bars, two independent batches), *LBD37* OXs (white bars, two independent lines) and *LBD38* OXs (grey bars, two independent lines). **(A)** Cyanidin glycoside A11. **(B)** Cyanidin glycoside A9. **(C)** Quercetin glycoside F6. **(D)** Quercetin glycoside F5. **(E)** Kaempferol glycoside F3. **(F)** Kaempferol glycoside F2 or F4. **(G)** Kaempferol glycoside F1. Results are mean values \pm standard deviations from three biological replicates for each genotype. For more details about structure and naming of these cyanidin- and flavonol-glycosides see legend to Figure 4 and Tohge *et al.* (2005). **(H)** Phloroglucinol staining of stem cross-sections of four-week-old WT and *LBD* OX lines. Bar = 0.5 mm.



Supplemental Figure 5. Expression of late flavonoid pathway genes and regulators in *lbd37*, *lbd38* and *lbd39* mutants.

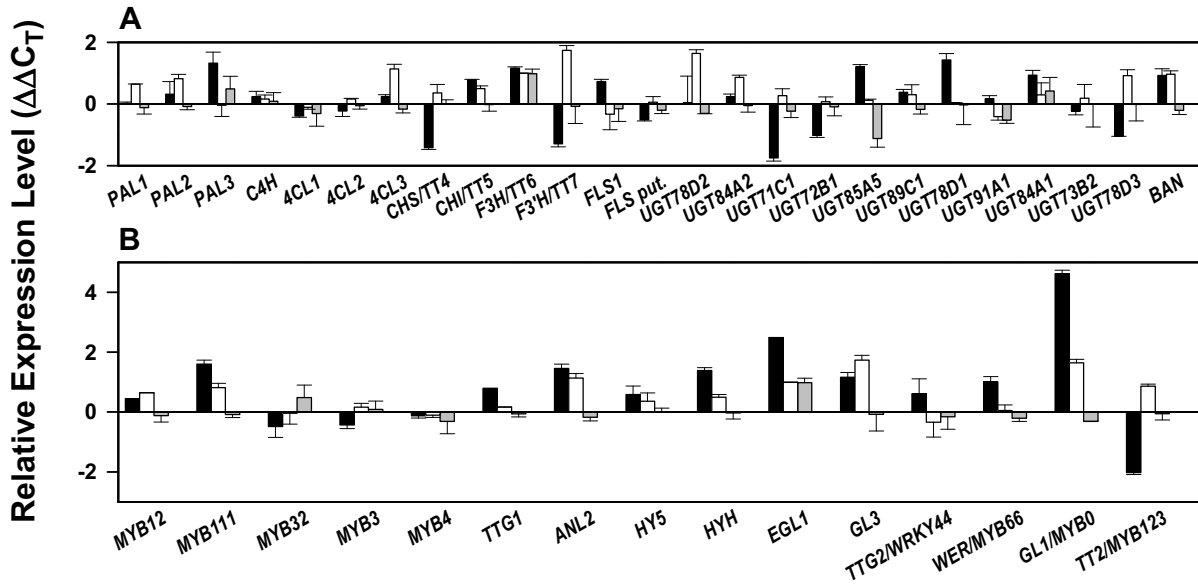
(A) Relative expression levels are shown for NO₃⁻-sufficient *lbd37-1*, *lbd37-2*, *lbd38* and *lbd39* mutant seedlings (blue, dark blue, red and green bars, respectively) versus NO₃⁻-sufficient WT seedlings. **(B)** Relative expression levels (*lbd37-1*, *lbd38* and *lbd39* mutant (blue, red and green bars, respectively) versus WT) in seedlings grown in N-limitation and resupplied with 3 mM NO₃⁻ for 30 min. Note the logarithmic character of the y-axis, where e.g. a $\Delta\Delta C_T = 2$ equals a $(1+E)^2$ -fold change in expression, depending on primer efficiency (E) (cf. Supplemental Table 1). Results represent mean values \pm standard deviation from three independent biological replicates with two technical replicates for each.



Supplemental Figure 6. QRT-PCR transcript profiling of early flavonoid pathway genes and regulators.

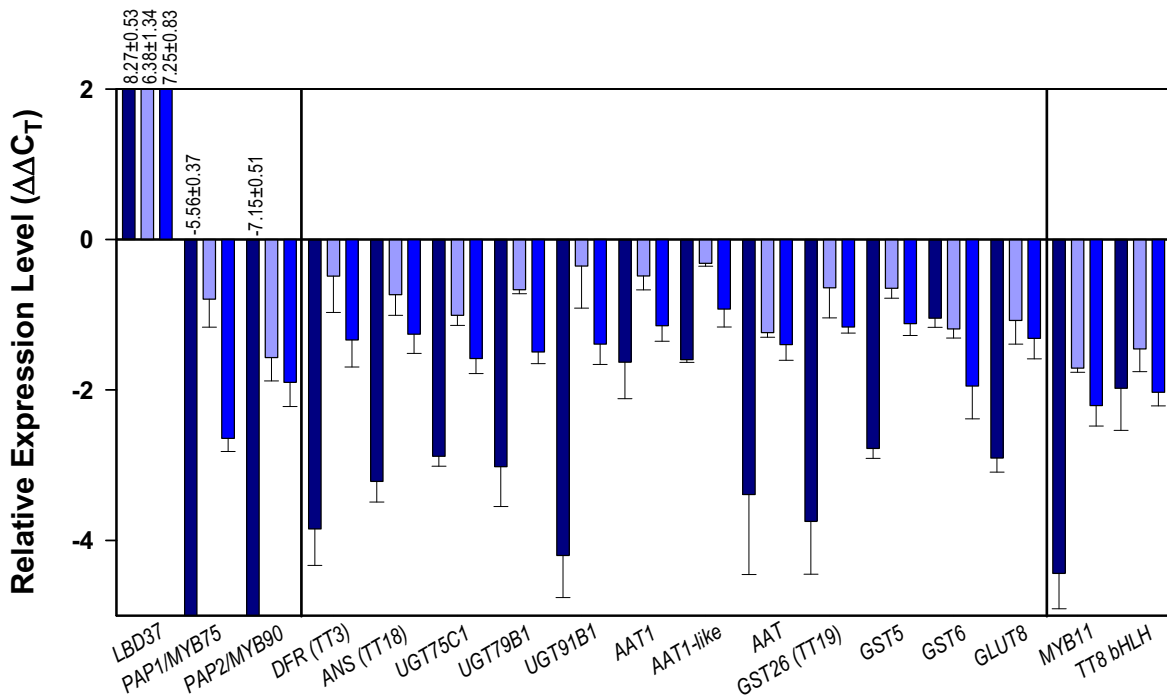
(A) Phenylpropanoid and early flavonoid pathway genes. **(B)** Regulatory genes.

Shown are relative expression changes in NO_3^- -fed versus N-limited WT (black bars), in the NO_3^- -fed *PAP1* over-expressing *pap1-D* activation tagging line versus NO_3^- -fed WT (white bars) and in N-limited over-expressers of *LBD37* versus N-limited WT (grey bars). Results represent mean values \pm standard deviation from three independent biological replicates with two technical replicates for each. Note the logarithmic character of the y-axis.



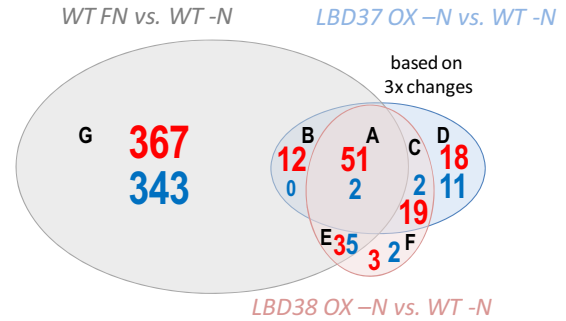
Supplemental Figure 7. Expression of flavonoid pathway genes and regulators in inducible *LBD37* OX lines.

Relative expression levels are shown for N-limited constitutive *LBD37* over-expressers versus N-limited WT seedlings (dark blue bars), N-limited inducible *LBD37* over-expressers (iOX) 3 hours after EtOH induction versus N-limited non-induced *LBD37* iOX (light blue bars), and N-limited inducible *LBD37* over-expressers (iOX) 6 hours after EtOH induction versus N-limited non-induced *LBD37* iOX (blue bars). Results represent mean values \pm standard deviation from three independent biological replicates/lines with two technical replicates for each. Note the logarithmic character of the y-axis.

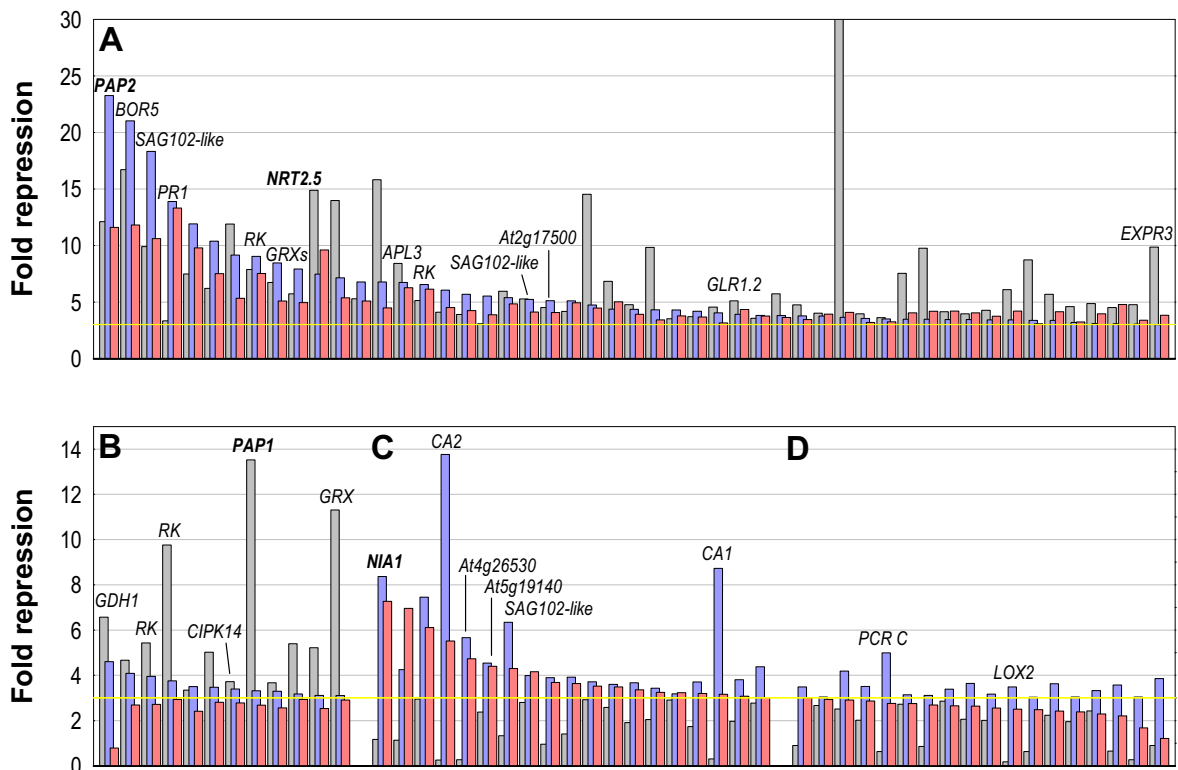


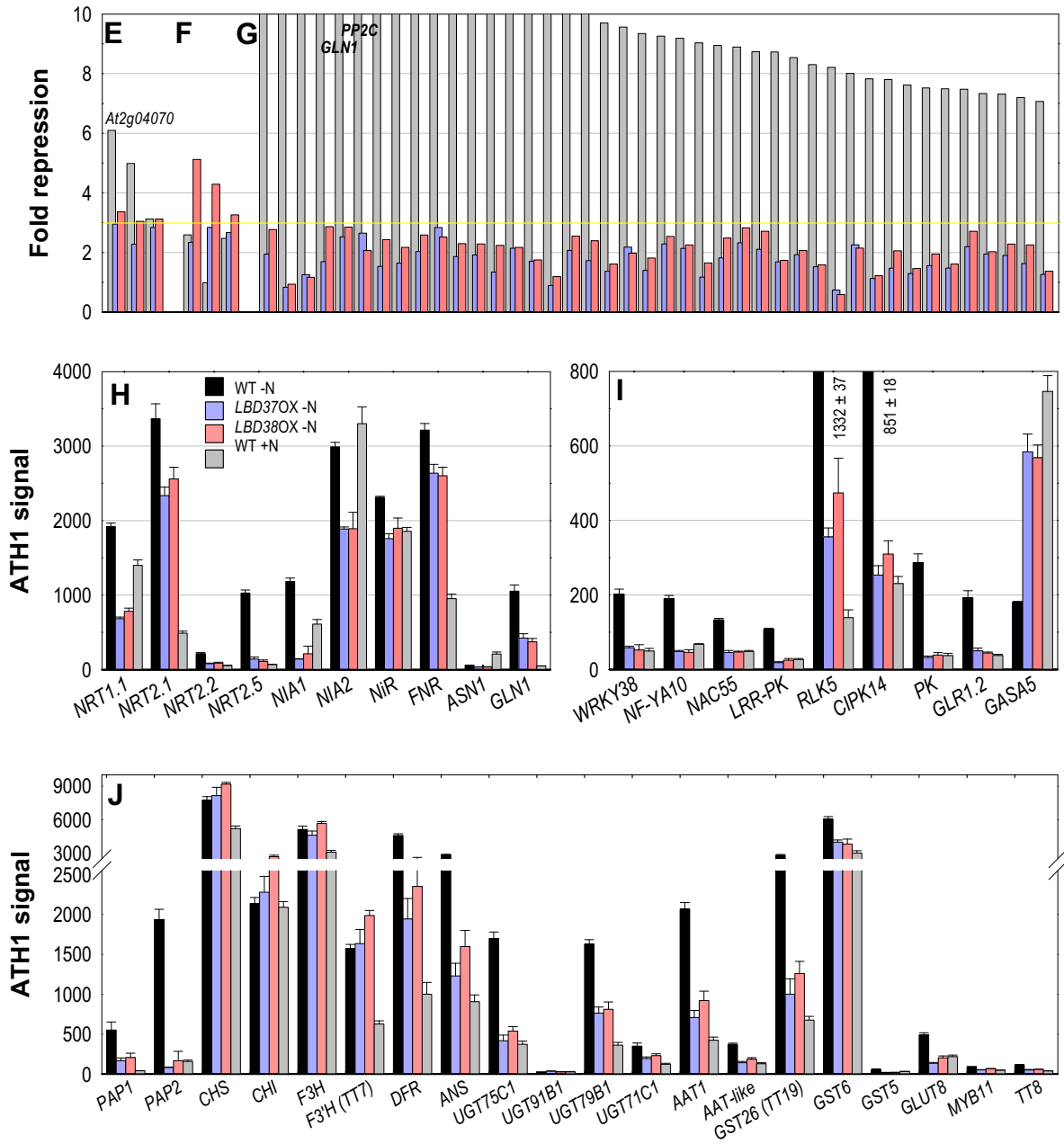
Supplemental Figure 8. Comparison of transcriptome changes in response to nitrogen status and *LBD37* or *LBD38* over-expression.

Shown in the Venn diagram (cf. Figure 7) are the numbers of gene transcripts that are ≥ 3 -fold decreased (red numbers) or increased (blue numbers) in either N-limited *LBD37* (light red) or *LBD38* (light blue) OX seedlings or N-replete WT seedlings (grey) compared to N-limited WT seedlings. Data were calculated from the average



of three biological replicates for each condition (Supplemental Datasets 1 and 2 online). The sizes of the ellipses are chosen to be roughly proportional to the number of affected transcripts. Average responses of repressed genes (red numbers) from the seven sectors (A-G) of the Venn diagram are depicted in panels A-G, respectively. Selected genes are labeled. Only a small number of genes from sector G are depicted. Yellow lines indicate the threshold for three-fold repression. (H-J) RMA-normalized ATH1 hybridization signals of (H) genes involved in nitrate uptake and assimilation, (I) potential regulatory genes, and (J) genes involved in anthocyanin biosynthesis. Mean values \pm standard errors (n=3) are shown.

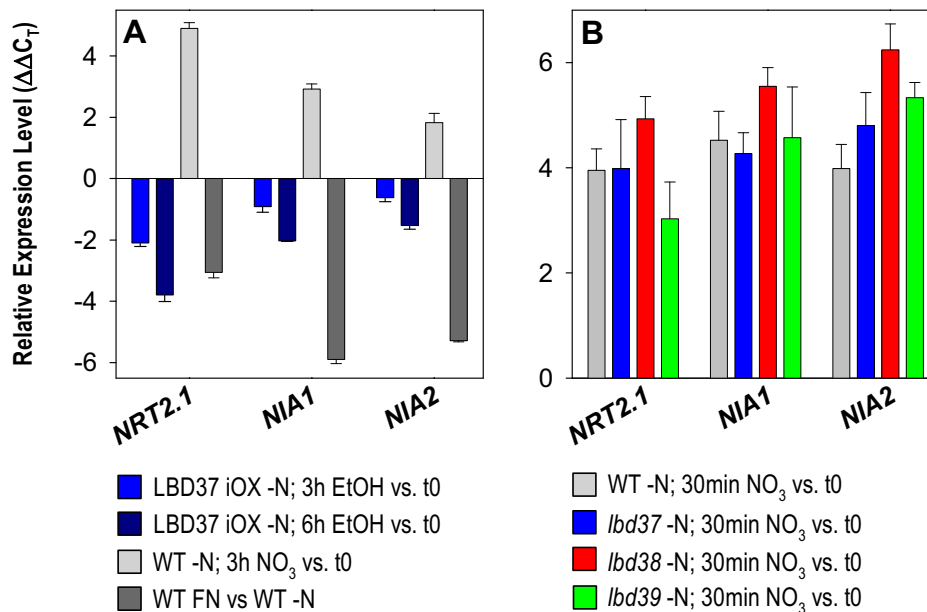




Supplemental Figure 9. Expression of *NRT2.1* and *NIA* genes in *LBD37* iOX lines and *lbd* mutant seedlings.

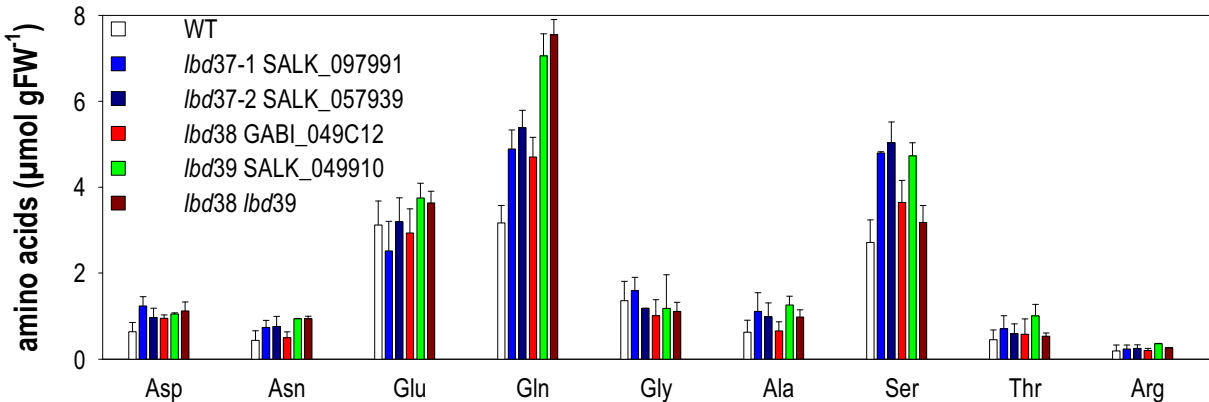
Shown are **(A)** relative expression levels of *NRT2.1*, *NIA1* and *NIA2* in N-limited ethanol-inducible *LBD37* over-expresser seedlings after 3 and 6 hours 0.2 % ethanol induction relative to N-limited ethanol-inducible *LBD37* over-expresser seedlings before induction (t0) (see graph for color explanation). For comparison the expression levels are also depicted for N-limited WT 3 hours after 3 mM KNO_3 re-addition and during continuous growth in N-replete (FN) conditions relative to N-limited WT. **(B)** Relative expression levels of *NRT2.1*, *NIA1* and *NIA2* in WT and *lbd* mutant seedlings grown in N-limitation and resupplied with 3 mM NO_3^- for 30 min.

Note the logarithmic character of the y-axis, where e.g. a $\Delta\Delta C_T = 2$ equals a $(1+E)^2$ -fold change in expression, depending on primer efficiency (E) (cf. Supplemental Table 1). Results represent mean values \pm standard deviation from three independent biological replicates with two technical replicates for each.



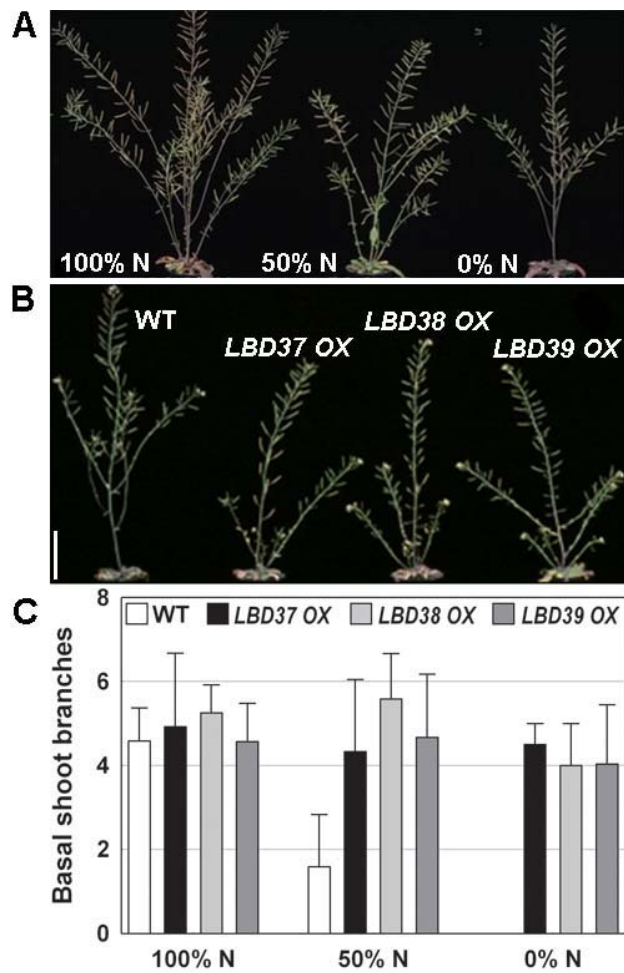
Supplemental Figure 10. Amino acid levels in *lbd* mutants as determined by HPLC.

Each bar shows the average \pm SD of three biological replicates from 9 day-old N-replete WT or *lbd* mutant shoots. The color legend is shown in the graph.



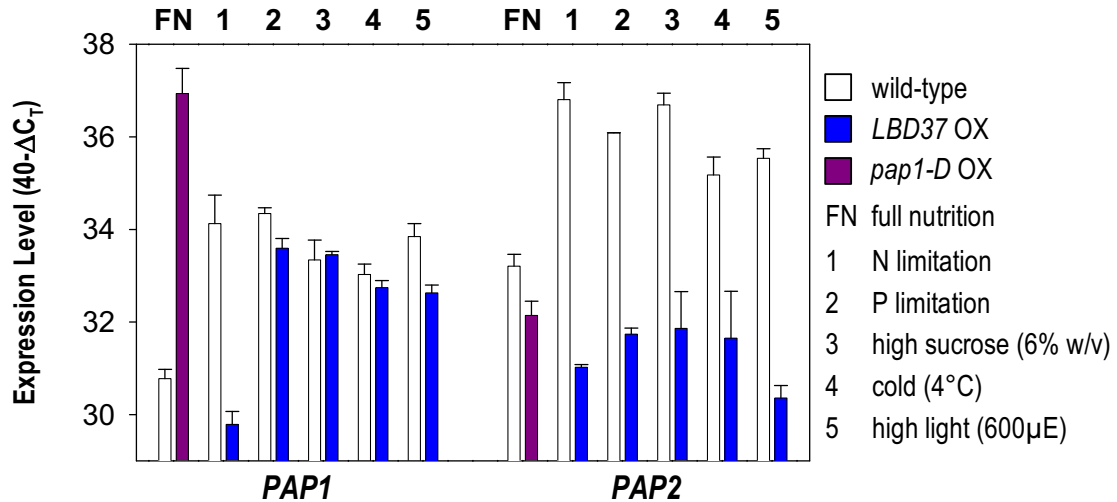
Supplemental Figure 11. Nitrogen-dependent basal shoot branching phenotype.

(A) N-dependent shoot branching of WT Col-0. (B) Shoot branching of WT, *LBD37*, *LBD38* and *LBD39* OX in N-limitation conditions (0% N). Bar = 5 cm in (A) and (B). (C) Plot of the number of basal shoot branches of wild-type, *LBD37*, *LBD38* and *LBD39* OXs against soil N-content (100% = 0.3 g $\text{NH}_4\text{NO}_3 \text{ l}^{-1}$ soil; cf. Method section). Results represent mean values \pm standard deviations (n=20).



Supplemental Figure 12. Expression of *PAP1* and *PAP2* in *LBD37* over-expressers during environmental stress conditions.

Shown are the expression levels of *PAP1* and *PAP2* in WT (white bars) and *LBD37* over-expresser seedlings (blue bars) subjected to N-limitation (1), P-limitation (2), high sucrose (6% w/v; 3), cold (4°C; 4) or high light (5). Results for nutrient-replete (FN) WT and *pap1-D* over-expression lines (purple bars) are shown for comparison. Expression levels are given on a log scale expressed as $40-\Delta C_T$, (cf. legend to Supplemental Figure 9). The results are the mean \pm SD of three independent biological replicates/lines with two technical replicates for each.



Supplemental Table 1. Accession numbers and primer sequences for (semi-) quantitative RT-PCR.

AGI	Gene Name	Forward Primer	Reverse Primer	Primer* efficiency
AT5G67420	LBD37	TGCTTTGTTTCAGTCGTTGCTC	TGCTCCGTTAACTGGATTGACA	2.00
	37a (cf. Fig. 2)	ACACCGTCGATGAACTCAGAGG	TGTCACAAAACGCCGTCGT	1.95
	37b (cf. Fig. 2)	CCCACCATTAACCAATTGTAAAACCT	GGATGCGTAACTATTTTGAGTTTATTCA	1.94
	37c (cf. Fig. 2)	XXXCTGCAATGGTTGCC	YYTAACAAAAAGGTTAAGCAAGT	n.a.
AT3G49940	LBD38	TGCCCTGCTTTGTTTCAGTCTT	CGTTCACCGGATTACAGTTCT	1.90
	38a (cf. Fig. 2)	TCACTGCCGATTCTCAAGCTC	GAGAGATCAAGCTCCGACGAA	1.93
	38b (cf. Fig. 2)	XXXTTGCAATGGTTGCGA	YYYCAAGCGAAGAGATTGAGCAA	n.a.
AT4G37540	LBD39 (39a)	GAACTCCAACGTCCTGCTTTGT	ATACCAACCGCTCCGTTAACC	1.90
	39b (cf. Fig. 2)	XXXTTGCAATGGATGTAGA	YYTAACAAAAAGGTTCAATAACTT	n.a.
AT1G02860	NLA	n.a.	n.a.	n.a.
AT1G02930	GST6	ACACAGGCTTGGTGAGTCCAA	GCAACCCAAGCACTCACATGT	1.77
AT1G02940	GST5	GTGAATGAAACCGAGGCGAAG	CGCTTGCCGGTTTACAAA	1.81
AT1G03495	AAT1-like	TTGGCAACTGTATGGCTCCTG	GCAGCCATGACGCATTTTTTC	1.94
AT1G03940	AAT1	AACAAAGGCCAACGAGGAAGA	CAGGAGCCATACAGTTGCCAA	1.88
AT1G06000	UGT89C1	TTCTTTAACACGACGCTCATCG	CAAATCCTAGCGAGCTTGTC	1.90
AT1G08090	NRT2.1	TTGCTTTCTCGTGCAATCAC	TGCTCTGTGTCCACCGGAA	1.99
AT1G08100	NRT2.2	GGAAAGATTCTATGGTACGCCG	CGGCATAACATTGTCTGTGC	1.86
AT1G12110	NRT1.1	CTGCCACACACTGAACAATTCC	CCCGCTTCTGATCCCTTAT	1.90
AT1G12940	NRT2;5	CGTTCTCTTGTTCGGTCAGGAT	TCCAGATTTATGCATCGCCC	1.85
AT1G22370	UGT85A5	AGATCGGTGGAGATGTGAGGA	TGCCACTCTTCGGCCTTTT	1.83
AT1G22640	MYB3	CTCCATAGCTTGTCCGTAACAA	CTGTTCTTCTGGTAATCTCCCAG	1.62
AT1G30530	UGT78D1	TGCTGAAACACGAGGCAATG	ATCCGCCAAAATCGGTCTG	1.98
AT1G34790	TT1	GCGATTGGCGAACACATGA	CCCAAACGCCTTAATACATGGTC	1.80
AT1G37130	NIA2	GCCGACGAAGAAGTTGGTGGTAT	GAAGAATCTCCTCGTGACATGGCG	1.99
AT1G51680	4CL1	CGGCTGAGCTAGAGGCTTTG	TCATTGCGACAACAGCAACAT	2.00
AT1G56650	PAP1/MYB75	TGCTGGAAGATTACCTGGTCCG	AGTGCCCGTGTGTAGGAATG	2.00
AT1G61720	BAN	CCGTGATTCCGGCACTTATAG	TCACATGCATTTCTTTCCCG	2.00
AT1G63650	EGL1/3	CATCAGCTAATACTCGGACCCG	TCTGCGATTTCTCTCCCAATGT	1.93
AT1G65060	4CL3	GCTGTTGTTCCGCAAAATGA	GAACACCACCTGTTTGCAA	2.00
AT1G66390	PAP2/MYB90	TCCTTCATGCCTTGGACTCAA	CAAAGTGCCCATGTTCA	1.96
AT1G77760	NIA1	GGCTACGCTTATTCTGGAGGAGGT	TGGTGGTCAAGCTCACAACACTC	1.90
AT2G22590	UGT91A1	GTTCTGACTCATCCCGTTGG	CCAGCATTGCCATCGGTTTA	1.90
AT2G29750	UGT71C1	CGGAACAACAATAAACGCGT	AACGGTTCCTGCGATCTCATC	1.83
AT2G30490	C4H	TGGTGTGGACGTCGAAGC	CCTACCAATGGTGATCCCA	1.95
AT2G37040	PAL1	CTTGAACAGAGCTTTTGACCG	CGTGAAAACCTTGTCGAATCTTC	1.91
AT2G37260	TTG2/WRKY44	CGGTTGCAAGAGTAGCCAATG	CCTTGCGATACTCCTGCTTCA	1.90
AT2G47460	MYB12	AACAGGTGGTCACTAATCGCG	TTCTGTTGCTGTTCTCCCTGG	1.97
AT3G17609	HYH/bZIP	CTGCAGCTGGATCAACATGTGT	GCGGCGTTTAGCTGTAGAGACT	1.89
AT3G21240	4CL2	TGATGTTGCTGTCGTCGCC	CCACAAACGCAACAGGAACC	1.97
AT3G21560	UGT84A2	TGTGGATGGAACCAACGATG	TCACTCCCGTCTTCCAAACAT	1.91
AT3G27920	GL1/MYB0	CCGTGATTGTTCACTACTGCC	GCTGATACGACCGGTTAAAG	1.87

AT3G29590	AAT	TGTGTGCGTTGGTTTTGCAT	GCTTTCACGTGCGAAATCTCCC	2.00
AT3G50210	FLS putative	CGTTTGTTTGCAACATCGGT	CCGCGTCGAAGTTAGTCTCAT	1.86
AT3G51240	F3H/TT6	GCTACAAGACCAAGTCGGTGA	GCTCAAAAATGGCCGTGG	1.89
AT3G53260	PAL2	AACTGCGCCGATTCTAACC	TTCCAAGCTCTCCCTCACG	1.90
AT3G55120	CHI/TT5	CTCTCTTACGGTTGCGTTTTCG	CACCGTCTTCCCGATGATAGA	1.89
AT3G62610	MYB11	GGCGATTGTAACCCAAGCATT	TCACATGAGGACACGTGGACA	1.89
AT4G00730	ANL2/HD	AACGAACGGATGAGATGCGA	TCATTGCATTGGAGCGGAG	1.85
AT4G01070	UGT72B1	GTGAAGATATTCGTGCGGCAC	CCTTTGCCTTCTCACCTTCC	1.84
AT4G04750	GLUT8	TGGAGGCGTTTTAGGTGTTTTG	CCCAGCAATTGTTCTTCTGCA	1.90
AT4G05320	UBQ10	GGCCTTGATAATCCCTGATGAATAAG	AAAGAGATAACAGGAACGGAAACATAGT	2.00
AT4G09820	bHLH TT8	TGGAGACACCATTGCGTACGT	TCTTACAAGTACGCGTCCGCT	1.83
AT4G14090	UGT75C1	TTTTGGCGCATTGTGCTGT	TCAGCAAACCTGCGGAAACG	1.79
AT4G15480	UGT84A1	ATTGGTGCCACACAAGAGCAA	CCGGAACACCTGAAGACAAAGA	1.95
AT4G22870	ANS/TT18	GGCTGTGTTTTGTGAGCCACCA	CCTTGGAGGAAACTTAGCCGAGA	1.83
AT4G34135	UGT73B2	ATACTTGACCACCAAGCAACCG	TCCTACAGGCCATGTCACCATT	1.92
AT4G34990	MYB32	GGCAAGACAAGCTCCATGATG	ACAGCTACACTCCTTGCCGTTC	1.96
AT4G38620	MYB4	GCCACGTGTTTCAAGTGCA	TCCATTGCTCATGTCACCTCCC	1.87
AT5G04230	PAL3	ATCCGCTGTACCGGTTTGTG	TCTCCCGGTGACCGAACAT	1.84
AT5G07990	F3H/TT7	TTCTTACCTTCAGGCGTTATC	CGAGAGTGGTGTGGTGGATG	1.91
AT5G08640	FLS1	TTCTGAGGTTGAGTAATGGGAGG	CCGTCGTCCTATGCAACACAT	1.93
AT5G11260	HY5bZIP	TAGAGAATCTGGATCGGCGACC	CTCAACAACCTTTCAGCCGCT	1.85
AT5G13110	G6PD2	ACAAATCCCCGGAACATGCCTGA	CACTACACACCAGGAGTGCAGAGA	1.85
AT5G13930	CHS/TT4	GGAGAAGTTCAAGCGCATGTG	ATGTGACGTTTCCGAATTGTCG	1.97
AT5G14750	WER/MYB66	TCACCGAGCAAGAAGAGGATCT	CACCTGATTATCCGTTCCGACCC	1.92
AT5G16570	GLN1;4	GGCCAACTACCGGCCACTTAATA	TGTCGCCGAAGAAACATGGTACG	1.79
AT5G17030	UGT78D3	ATACTTGACCACCAAGCAACCG	TCCTACAGGCCATGTCACCATT	1.82
AT5G17050	UGT78D2	CGGTGTTGGAGAGTGTATCGG	TGATCCCCAAAAATGGCC	1.90
AT5G17220	GST26/TT19	TGGCTGATTTGACGCACATG	CCCAGCCTTAACCATCTGG	1.90
AT5G24520	TTG1/WD40	TCGATATTCGTTCCCGACT	GCCTGTGTATCATCACCACCAG	2.00
AT5G35550	TT2/MYB123	CCGCAAAAGACTTCCCAAAA	GCACCTAATCGCCTTTGTACGT	1.95
AT5G41315	GL3	TCGGTTCGTTTGGTAATGAGG	GCTTGCAATTGACGGTTAAGC	1.83
AT5G42800	DFR/TT3	CGTTTGAAGGTGTTGATGAGAATC	TCCGTCAGCTTCTTGGAAGT	1.95
AT5G49330	MYB111	CGGCCTCACAATGTTTCTCAC	CCACTCATAAGGCCCAAAGA	1.88
AT5G54060	UGT79B1	CAGCAACCGTTGGTGTGAAC	GCGGAACCAAAACGATCTGAC	1.95
AT5G65550	UGT 91B1	AGCCATGGTTCAGTTGGTGG	CACCAAAGCTAAGCCCTTCCA	1.87

*Primer efficiency was determined using LinRegPCR (Ramakers *et al.*, 2003).

XXX = GGAGATAGAACCATGAG; YYY = CAAGAAAGCTGGGTCT. Primers for semi-quantitative PCR (cf. Figure 2C, D) are shown in grey letters. n.a. = not applicable/analyzed.